

Initial Growth and Oxygen Adsorption of Silver on Al₂O₃ Film

Donghui Guo,[†] Qinlin Guo,^{*,†} Kefei Zheng,[†] E. G. Wang,[†] and Xinhe Bao[‡]

Beijing National Laboratory for Condensed Matter Physics, Institute of Physics, Chinese Academy of Sciences, P. O. Box 603, Beijing 100080, China, and State Key Laboratory of Catalysis, Dalian Institute of Chemical Physics, Chinese Academy of Sciences, Dalian 116023, China

Received: October 18, 2006; In Final Form: January 12, 2007

The growth and oxygen adsorption of Ag on an ordered Al₂O₃ film, prepared on Mo(110) substrate, have been studied in situ under ultrahigh-vacuum condition using X-ray photoelectron spectroscopy, ultraviolet photoelectron spectroscopy, and low-energy electron diffraction. The results show that Ag particles/clusters are formed on alumina film at initial coverages, and the binding energy of the Ag 3d_{5/2} line for Ag clusters is higher than that of bulk Ag, arisen from the size effect. Exposure of Ag clusters to $\sim 10^{-7}$ mbar O₂ leads the clusters to spreading over the substrate. It is of importance in many application areas to understand the origin of oxygen-induced metal-cluster changes in morphology and size.

1. Introduction

Metal clusters/particles have received considerable attention due to their tremendous importance in both fundamental research and applications, for instance, in heterogeneous catalysts. A metal cluster represents an intermediate state of matter between isolated atoms and bulk material, involved in the transition from the discrete energy levels of free atoms to the continuous energy band of bulk metals. Many noble metals, chemically inert in bulk form, are active chemically in clusters. For instance, small Ag clusters supported on oxides have been used as catalysts for selective oxidation for ethylene and formaldehyde,^{1–5} and for lean-NO_x reaction.^{6,7}

Due to the complexity of real catalysts used in the industry, it is difficult to understand their catalytic processes in detail. For the sake of model catalysts with consideration of bulklike property, ordered metal oxide films have been prepared under ultrahigh-vacuum conditions. Thus, the metal clusters supported on oxide films, including Ag clusters supported on Al₂O₃, have been investigated extensively.^{8–19} The previous studies were mainly focused on the Ag growth mode and interaction between Ag and oxide substrate, as well as desorption temperature of Ag. A recent study has reported that under oxygen-rich conditions, some transition metal catalysts may be covered by thin “surface-oxide” overlayers and found to be catalytically more active than the pure metal surface that was traditionally assumed.²⁰

In this work, we present our recent studies on Ag supported on an ordered alumina film, which was prepared in situ on Mo(110) substrate, followed by exposure to oxygen. The experiments were performed in ultrahigh-vacuum using X-ray photoelectron spectroscopy (XPS), ultraviolet photoelectron spectroscopy (UPS), and low-energy electron diffraction (LEED). The results show a formation of Ag clusters at initial coverages of Ag on alumina films. The binding energy (BE) shift of Ag 3d_{5/2} core level at initial Ag coverage shows cluster size

dependence. The exposure of supported Ag clusters to oxygen leads to a formation of smaller clusters spreading over the alumina substrate.

2. Experiment

The experiments were carried out in an ultrahigh-vacuum system (ESCA-LAB 5, VG Scientific Ltd., U.K.), which is equipped with reverse view optics for LEED, dual-anode X-ray sources (Mg and Al) for XPS, a He(I) source for UPS and various sources, including aluminum, silver, and oxygen. The base pressure of the ultrahigh-vacuum system was 2×10^{-10} mbar.

The Mo(110) substrate (a 10 mm diameter disk with thickness of 0.5 mm) was fixed to the manipulator with a Ta wire spot-welded to its edge. Temperatures were monitored with a thermocouple (W–5%Re/W–26%Re) spot-welded to the edge of the Mo(110) crystal. An e-beam heater was assembled at the rear side of the Mo sample which provided capability for heating to 2500 K. Prior to the growth of alumina film, the Mo(110) substrate was cleaned by heating to ~ 2000 K, then annealed at 1200 K in 8×10^{-8} mbar O₂ subsequently followed by flash to ~ 2000 K to remove surface oxide. After several cycles of such treatment, a well-ordered (1 × 1) LEED pattern with sharp spots was obtained, and no impurity was detected by XPS.

The aluminum source was made of high-purity (99.999%) aluminum wire filled in a high-purity alumina tube. The tube was heated by a tungsten wire. A resistively heated tungsten wire wrapped with Ag wire, purity of 99.99%, was used for the silver source. Aluminum and silver sources were thoroughly degassed before deposition.

The ordered alumina film was synthesized in ultrahigh-vacuum by exposing the Mo(110) surface to Al vapor in 8×10^{-8} mbar O₂ ambience at ~ 600 K followed by annealing under the same temperature and O₂ pressure to enhance oxidation. Then the film was annealed to 1150 K without O₂ for surface ordering before characterization by LEED, XPS, and UPS. A typical thickness of the alumina film is 3–5 nm.

The deposition rate of Ag was carefully calibrated via Ag/Mo XPS intensity ratio versus the Ag deposition time. Since

* To whom all correspondence should be addressed. E-mail: qlguo@aphy.iphy.ac.cn.

[†] Institute of Physics.

[‡] Dalian Institute of Chemical Physics.

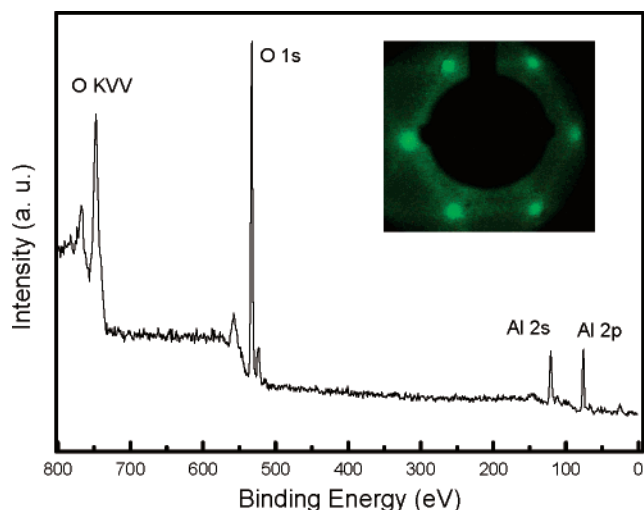


Figure 1. XPS spectra and LEED pattern (inset, $E_p = 86$ eV) of Al_2O_3 film on $\text{Mo}(110)$.

the Ag is not necessarily grown on alumina as a layer-by-layer mode, we prefer to use monolayer equivalent (MLE) as a unit of the amount of Ag deposition (1 MLE = 1.4×10^{15} atoms/cm² for Ag(111) and 1.2×10^{15} atoms/cm² for Ag(100)). All depositions of Ag were carried out at room temperature (RT). The oxygen dose was taken from uncorrected ion gauge reading. XPS measurements were performed using the Mg K α (1253.6 eV) X-ray source. The BE was carefully calibrated by a standard method using pure metallic Au (4f_{7/2}, BE = 84.0 eV) and Cu (2p_{3/2}, BE = 932.7 eV). All data were recorded at RT.

3. Results

Figure 1 shows the results of XPS and LEED for an ordered Al_2O_3 film grown upon $\text{Mo}(110)$ in ultrahigh-vacuum. The BE of Al 2p line is 76.0 eV, agreeing well with that of stoichiometric Al_2O_3 films.^{21,22} We noticed that the BE of Al 2p is higher than the bulk Al_2O_3 in literature.²³ This BE shift is not caused by surface charging effect, but a film thickness-dependent effect as observed previously.²¹ From the LEED, a hexagonal pattern of the Al_2O_3 surface (inset in Figure 1) was obtained, indicating either a (0001) surface of α - Al_2O_3 or a (111) orientation of γ - Al_2O_3 .^{24,25} Then, the Ag was deposited on the ordered alumina film in situ at RT and followed exposure of oxygen with different oxygen pressure and the temperature.

From a clean alumina film, the BE of the O 1s line is 532.9 eV. After deposition of 1 MLE of Ag, the BEs of O 1s and Al 2p lines from substrate are shifted to 532.8 and 75.9 eV, respectively. At this initial coverage, the BE of Ag 3d_{5/2} is located at 369.4 eV as shown in Figure 2a, 1.1 eV higher than that of metallic Ag.²³ After exposure of the 1 MLE Ag/ Al_2O_3 to 8×10^{-7} mbar oxygen at RT for 15 min, the BE of Ag 3d_{5/2} shifts to 369.9 eV (Figure 2b), and the BE of O 1s and Al 2p are shifted to 532.7 and 75.8 eV, respectively. The BEs of O 1s and Ag 3d_{5/2} were not changed with further oxygen exposure at RT (see Figure 2c). More oxygen exposure at 700 K for 30 min does not change the BE value of O 1s, but the Ag 3d_{5/2} core level peak is shifted to 370.1 eV as seen in Figure 2d.

The change of BE of Ag 3d_{5/2} with different coverage before and after exposure of oxygen is shown in Figure 3. By increasing Ag coverage from 0.5 to 5 MLE, the value of BE decreases from 369.4 to 368.7 eV. The results clearly reveal that at RT the BE is changed as a function of Ag coverage. After exposure

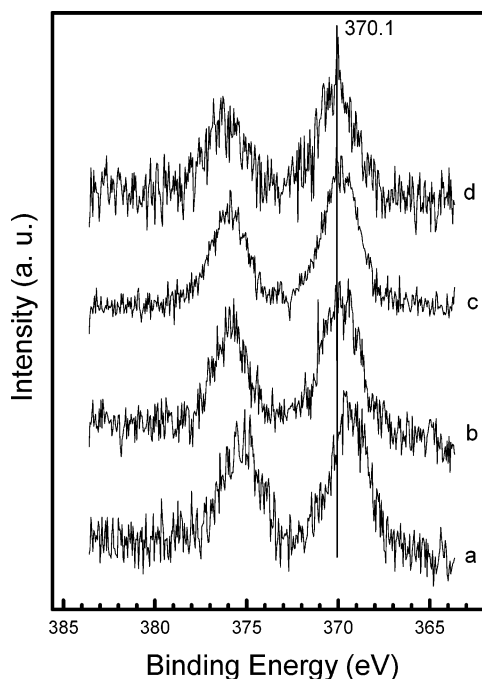


Figure 2. XPS spectra of Ag 3d: (a) 1 MLE Ag deposited on Al_2O_3 film; (b) a after 8×10^{-7} mbar oxygen for 15 min at RT; (c) a after 8×10^{-7} mbar oxygen for 30 min at RT; (d) a after 8×10^{-7} mbar oxygen for 30 min at 700 K. The vertical line indicates the Ag 3d_{5/2} position of 370.1 eV.

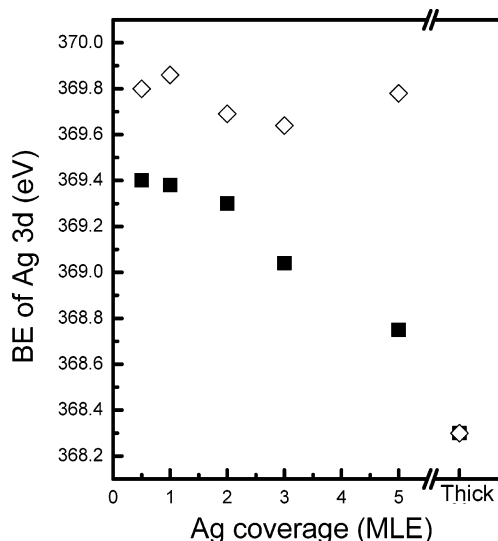


Figure 3. Changes of BE of the Ag 3d_{5/2} level as a function of Ag coverage before and after exposure to $\sim 10^{-7}$ mbar O_2 at RT for 15 min each step: (■) before oxygen exposure; (□) after oxygen exposure.

of the samples to 8×10^{-7} mbar oxygen at RT, the BEs of Ag 3d_{5/2} shift to the values in the range from 369.6 to 369.9 eV. For a thick Ag (>60 MLE) on Al_2O_3 , its BE is 368.3 eV, characterizing a typical feature of metallic Ag.²³ However, it is notable that this value is not changed after exposure of oxygen. This suggests that for an initially deposited Ag on alumina it is more chemically active than thick Ag.

In XPS measurements, the Auger parameter α , $\alpha = E_B(\text{XPS}) + E_K(\text{Auger})$, where E_B is the BE of the most intense core level photoemission peak and E_K is the kinetic energy of the most intense Auger transitions, can be used to distinguish chemical states of the element of interest and to differentiate the contributions of final and/or initial state effects.²⁶ In the case

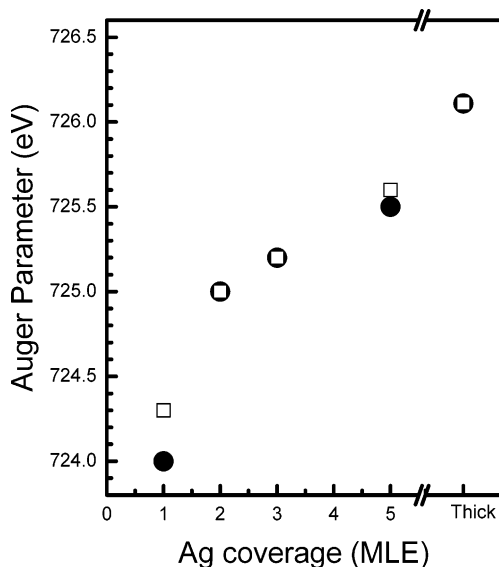


Figure 4. Changes of α of Ag as a function of Ag coverage before and after exposure in $\sim 10^{-7}$ mbar O₂ at RT for 15 min each step: (●) before oxygen exposure; (□) after oxygen exposure.

of Ag, however, the Ag 3d_{5/2} core level and M₄VV (the less intense Auger transition) are the lines cited because the M₄VV Auger line is narrower and more easily measured accurately than the M₅VV, the most intense Auger transition of Ag. In the literature, the α value is around 726 eV for a bulk Ag and in the range of 724–725 eV for Ag oxides.^{23,27,28} We monitored the change of the α as a function of Ag coverages before and after oxygen exposure. The value of the α increases from 724.0 to 725.5 eV with increasing coverage from 1 to 5 MEL (Figure 4) before oxygen exposure. This indicates convincingly that the α value is increased with an increase of coverage. After exposure of a sample with 1 MLE coverage to 8×10^{-7} mbar oxygen at RT for 15 min, the α value is shifted to 724.3 eV. For the samples with 2–5 MLE coverages, the values of the α are not obviously changed after O₂ exposure. The result from α measurement contrasts with that of the 3d core level energy shift, as shown in Figure 3. However, for a thick Ag, the α value is also not changed before and after oxygen exposure, consisting with the result of XPS, indicating that the thick Ag is not active as initially deposited Ag clusters is. This is in a good agreement with the results of prior work.²⁹

Figure 5 shows the UP spectra for a clean alumina film and Ag deposited on the film as a function of Ag coverage. A broad and unresolved peak in the range of BE from 5 to 14 eV features the valence band from a clean Al₂O₃ (bottom spectrum in Figure 5), comprised mainly of Al 3s and O 2p states.³⁰ With increasing Ag coverage, this broad peak is shifted to lower energy in BE. For a thick Ag, the dominated peak is at ~ 5 eV. The inset in Figure 5 shows the detailed spectra in the range 0 to 4 eV below Fermi level (E_F). The density of the state (DOS) near E_F is gradually increased with an increase of coverage of Ag. At initial depositions of Ag, no DOS near E_F appeared, demonstrating a nonmetallic Ag, due to small Ag particles formed on the surface of the alumina film (see below in Discussion). That continual increasing Ag coverage causes the DOS near E_F to be more intense, and a sharp Fermi edge can be observed from a sample with thick coverage, being character of the metallic Ag.³¹

Figure 6 shows the XPS results for 5 MLE Ag/Al₂O₃ after treatment in 8×10^{-7} mbar oxygen for 15 min at different temperatures. After exposure to O₂ at RT, the BE of Ag 3d_{5/2} is shifted from 368.8 eV (Figure 6a) to 369.7 eV (Figure 6b). No obvious changes of the Ag 3d_{5/2} line and α are observed at

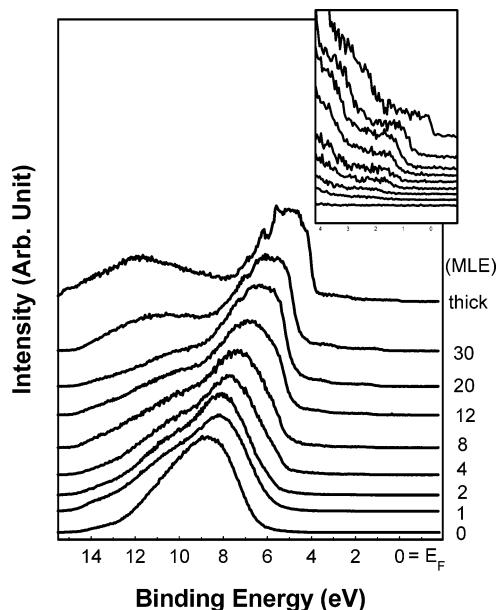


Figure 5. UP spectra of Ag/Al₂O₃ as a function of Ag coverage. The inset shows the detailed change from 0 to 4 eV.

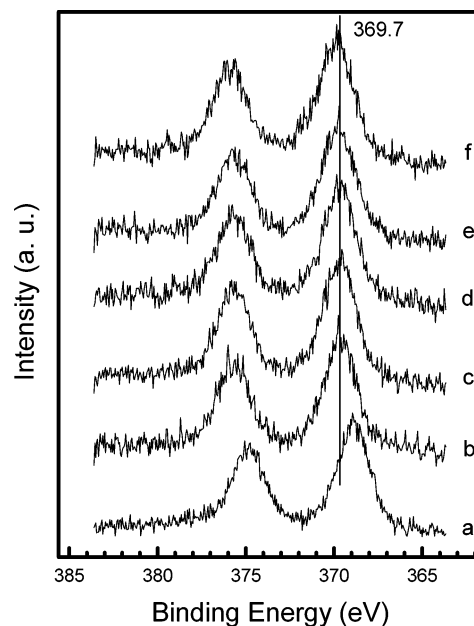


Figure 6. XPS of Ag 3d from 5 MLE Ag on the Al₂O₃ surface: (a) before oxygen exposure; (b–f) after 8×10^{-7} mbar oxygen for 15 min at RT, 400, 500, 600, and 700 K, respectively. The vertical line indicates Ag 3d_{5/2} position of 369.7 eV.

the temperatures less than 500 K (Figure 6c,d). A higher temperature treatment, 600 and 700 K, results in a slight shift of the 3d_{5/2} line to 369.8 eV, as shown in Figure 6e,f. After annealing the sample without oxygen at 850 K, the BE of Ag 3d_{5/2} is shifted back to lower value meaning that the oxygen-induced BE shift of Ag is partly reversible.

4. Discussion

Our results strongly suggest that the BE of Ag 3d_{5/2} is shifted as a function of Ag coverage. Several reasons are believed to result in a shift of core level peak in photoelectron emission spectroscopy, e.g., charging effect, chemical bonding, and size effect. For an insulator sample, it exhibits positive character during XPS measurement because negative electrons are emitted due to photoemission, which will cause all XPS lines to shift

to higher BE with the same value. In our experiments, the ultrathin film (<5 nm) of the alumina is prepared on a metal substrate, which can entirely circumvent the surface charging problem. Also, while the Ag 3d_{5/2} core level peak is shifted to higher BE after exposing Ag/Al₂O₃ to oxygen (Figure 2), the O 1s peak from the substrate is not shifted, meaning that in our case the charging effect takes no account.

A chemical bonding involving charge transfer after oxidation or reduction can result in a shift of BE. After exposing Ag/Al₂O₃ with small depositions of Ag, ≤ 5 MLE, to $\sim 10^{-7}$ mbar O₂ at RT, the peak of Ag 3d_{5/2} shifts to higher in BE, ranging from 369.6 to 369.9 eV (Figure 3). It is well-known that in the case of bulk Ag and Ag oxides, the shift of Ag 3d_{5/2} to higher BE implies a reduction.^{32–38} It seems that the BE shift to higher BE in Figure 3 is caused by a reduction of Ag clusters. Obviously, it is chemically unreasonable that Ag clusters are reduced in oxygen environment.

From previous studies, we know that the Ag is grown on the alumina as clusters, e.g., a formation of Ag clusters on alumina film has been observed by scanning tunneling microscopy (STM) technique.¹⁵ The BE shifts to higher value with decreasing size by $\Delta BE \sim 1$ eV from bulk metal to small clusters on insulating supports have been observed^{8,39,40} to be correlated with the quantum size effect due to initial state or/and final state.^{8,10,15,41,42} The contributions of initial state effect and final state effect are different; the former one is related to the real evolution of the electronic structure of the metal clusters, and the latter is related to the screening of the photoemission core hole which depends strongly on the cluster size and the shape as well as on the nature of the substrate.⁹

The contribution of the final state can be evaluated from α measurements. It has been found that the difference in the Auger parameter ($\Delta\alpha$) for a given element in two different environments is approximately twice the difference in final state effect (ΔR), $\Delta\alpha = 2\Delta R$.⁴³ In our experiments, the BE of Ag 3d_{5/2} from a sample with 1 MLE coverage is 1.1 eV higher than that of bulk Ag (Figure 2), and the $\Delta\alpha$ of Ag is 2.1 eV. From the equation above, we conclude that the shift of the core level BE of Ag is mainly contributed to the final state effect, which coincides with a previous study.¹⁵ We have also noticed that the initial state effect may originate from an interfacial chemical reaction. Since its interaction is weak between Ag and alumina,¹⁵ which further supports our result. As a matter of fact, the initial state contribution is only important for small clusters;⁹ this may mean that the clusters of the Ag on the alumina film in our study are not very small.

Similarly, the size-induced core level BE shifts for Cu and Sn, for instance, have been reported.^{44,45} Recent studies have been also shown that the extent of core level shift depends on both the original core level position of the isolated atom and the reduced particle size, and a quantitative bond order–length–strength (BOLS) correlation mechanism has been developed to elucidate the origin for core level BE shift caused by the reduced particle size.^{46–48} Using the BOLS model, the size-deduced BE shift can be calculated from the exact particle size and a set of XPS data. Although we do not know the exact size of the Ag particles in our study, it is obviously that the shift of the BE of Ag 3d_{5/2} is the size dependence of Ag clusters.

A detailed change in the valence band for the sample with a coverage of 3 MLE is presented in Figure 7. For a clean surface of alumina film, its valence band is empty from 0 to 4 eV (Figure 7a). An initial growth of Ag on alumina causes a new peak at about 1.8 eV below E_F , which is an evidence of a formation of Ag clusters due to size effect as discussed above.

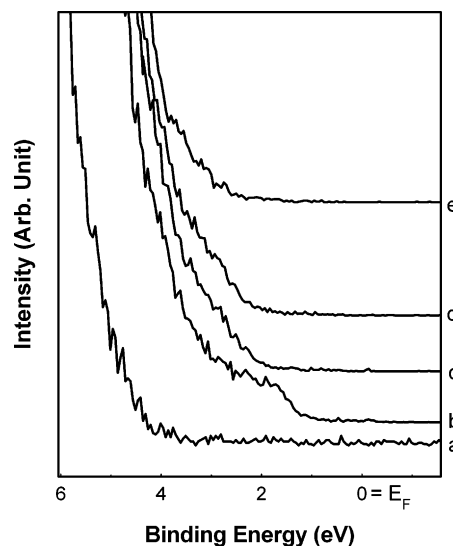


Figure 7. UP spectra from (a) clean Al₂O₃ film; (b) 3 MLE Ag deposited on Al₂O₃ film; (c) b after 8×10^{-7} mbar oxygen for 15 min at RT; (d) b after 8×10^{-7} mbar oxygen for 30 min at RT; (e) b after 8×10^{-7} mbar oxygen for 30 min at 700 K.

After exposure of oxygen at RT for 15 and 30 min, the peak at 1.8 eV is diminished (see Figure 7c,d). The oxygen adsorption of Ag depends on the different faces and the substrate temperature. For instance, in the case of oxygen adsorption on Ag(110), oxygen is chemisorbed in the temperature range between 40 and 150 K, and oxygen molecules dissociate at the temperature > 150 K.^{49,50} A previous UPS result from a single crystal of Ag(111) sample shows a sharp cure at E_F , a typical metallic Ag character.³¹ However, after exposure of oxygen, a new feature appears at 3 eV below E_F , and the intensity of the peak at E_F position is diminished due to an oxidation of Ag(111) surface.³¹ In our study, the disappearance of the peak of 1.8 eV after oxygen exposure suggests an oxidation of Ag. After 700 K oxidation, no obvious change of valence band was found (Figure 7e), implying the entire oxidation of Ag clusters.

Oxygen-induced particles change has been observed in other systems. For example, it was found that after Fe islands, grown on oxide substrate, were exposed to oxygen, a flat film was obtained.⁵¹ This has been explained as due to the fact that the metal oxides have significantly lower surface free energies than those of the metals; the oxygen-induced spreading of the Fe film is not caused simply by adsorption of oxygen, but by the oxidation of Fe. Also, that exposure of Cu and Ni clusters supported on TiO₂(110) to oxygen leads the Cu and Ni 3D clusters to decreasing into two-dimensional (2D) structure and oxidizing.^{52,53} Moreover, an initial oxidation of Pd nanoparticle on Fe₃O₄ in $\sim 10^{-6}$ mbar oxygen can result in a formation of a thin Pd oxide layer at the particle/support interface,^{54,55} and its oxidation mechanism gives rise to pronounced particle-size effects. Those studies are very similar to what as we found in the Ag/Al₂O₃ system. The morphology of Ag or Ag oxide on alumina depends on the surface and interface free energy.^{56–58} For the system of Ag on alumina, the surface free energy of alumina (γ_{ox} , 0.69 J m⁻²), is lower than the sum of the surface free energy of Ag (γ_{Ag} , 1.3 J m⁻²), and the interface free energy of Ag/alumina ($\gamma_{Ag/ox}$, 0.69 J m⁻²),^{59–61} i.e. $\gamma_{ox} < (\gamma_{Ag} + \gamma_{Ag/ox})$, the Ag clusters form on alumina film. In case of Ag oxide on alumina, the surface free energies of Ag oxide are 0.28 J m⁻² for AgO and 0.33 J m⁻² for Ag_{1.83}O,²⁰ which are lower than that of Ag and Al₂O₃. Therefore, 2D Ag oxide growth mode is expected and thermodynamically favorable. A previous study

has been pointed out that the interaction between Ag clusters and alumina is weak,¹⁵ differing from that of Ag oxides on alumina.

Interestingly, at initial coverages, ≤ 5 MLE, the values of α are not changed obviously after O₂ exposure at RT, as shown in Figure 4. The energy shift of Auger electron is sensitive to the size of the clusters, the smaller Ag clusters cause the value to shift to lower energy in kinetic energy (higher BE). However, after O₂ exposure, the core level BE is shifted to higher value in XPS (see Figure 3). This makes a compromise between the shift of the Auger transition and the BE shift for the samples with a certain coverage, resulting in a nonshift of the α value.

The origin of the BE shift of the core level of Ag 3d to higher position after exposure of oxygen might be attributed to a size effect; i.e., it is most likely that the induced oxygen led AgO_x clusters to spread over the surface. A slight increase of the intensity ratio of Ag to Al in XPS after O₂ adsorption further proves that the AgO_x clusters become smaller. The clusters are thermally stable at the temperatures < 500 K, as monitored by XPS. Oxygen-induced metal particle changes in size and chemistry play an important role in many application areas. However, detailed studies on the morphological change of Ag clusters with oxygen exposure by STM or atomic force microscopy methods in situ are expected.

5. Conclusion

The growth and O₂ adsorption of Ag clusters on Al₂O₃ films have been studied in situ under ultrahigh-vacuum condition using surface analysis techniques. At initial coverages, less than 5 MLE of Ag on Al₂O₃ surface, the BE of Ag 3d_{5/2} is 0.4–1.1 eV higher than that of bulk Ag due to size effect. After exposure of oxygen, Ag clusters are oxidized and spread over the alumina surface, resulting in smaller particles. That the oxygen-induced morphology change in Ag/oxides observed in this study is widely existed in metal/oxide systems. The study on the origin of the BE changes as a function of metal oxide clusters in nanosize is important in many application areas, especially in catalysis.

Acknowledgment. We acknowledge with pleasure the support of this work by the National Science Foundation of China (Grants 90206036 and 10574153). We also thank Professor Preben J. Moller for critical reading of the manuscript.

References and Notes

- Mao, C.-F.; Vannice, M. A. *Appl. Catal., A* **1995**, *122*, 61.
- Bulushev, D. A.; Paukshtis, E. A.; Nogin, Y. N.; Balzhinimaev, B. S. *Appl. Catal., A* **1995**, *123*, 301.
- Bukhtiyarov, V. I.; Prosvirin, I. P.; Kvon, R. I.; Goncharova, S. N.; Balzhinimaev, B. S. *J. Chem. Soc., Faraday Trans.* **1997**, *93*, 2323.
- Lee, J. K.; Verykios, X. E.; Pitchai, R. *Appl. Catal.* **1989**, *50*, 171.
- Mao, C.-F.; Vannice, M. A. *J. Catal.* **1995**, *154*, 230.
- Bethke, K. A.; Kung, H. H. *J. Catal.* **1997**, *172*, 93.
- Hoost, T. E.; Kudla, R. J.; Collins, K. M.; Chattha, M. S. *Appl. Catal., B* **1997**, *13*, 59.
- Mason, M. G. *Phys. Rev. B* **1983**, *27*, 748.
- Henry, C. R. *Surf. Sci. Rep.* **1998**, *31*, 231.
- Bäumer, M.; Freund, H.-J. *Prog. Surf. Sci.* **1999**, *61*, 127.
- Lazzari, R.; Jupille, J. *Surf. Sci.* **2001**, *482–485*, 823.
- Zhang, W.; Smith, J. R. *Phys. Rev. Lett.* **2000**, *85*, 3225.
- Van Campen, D. G.; Hrbek, J. *J. Phys. Chem.* **1995**, *99*, 16389.
- Rodríguez, J. A.; Kuhn, M.; Hrbek, J. *J. Phys. Chem.* **1996**, *100*, 18240.
- Luo, K.; Lai, X.; Yi, C.-W.; Davis, K. A.; Gath, K. K.; Goodman, D. W. *J. Phys. Chem. B* **2005**, *109*, 4064.
- Zhukovskii, Yu. F.; Kotomin, E. A.; Herschend, B.; Hermansson, K.; Jacobs, P. W. M. *Surf. Sci.* **2002**, *513*, 343.
- Dligatch, S.; Cheary, R. W.; Smith, G. B. *Thin Solid Films* **1998**, *312*, 4.
- Lazzari, R.; Roux, S.; Simonsen, I.; Jupille, J.; Bedeaux, D.; Vlieger, J. *Phys. Rev. B* **2002**, *65*, 235424.
- Nilus, N.; Ernst, N.; Freund, H.-J. *Phys. Rev. Lett.* **2000**, *84*, 3994.
- Michaelides, A.; Reuter, K.; Scheffler, M. *J. Vac. Sci. Technol., A* **2005**, *23*, 1487.
- Wu, Y.; Tao, H.-S.; Garfunkel, E.; Madey, T. E.; Shinn, N. D. *Surf. Sci.* **1995**, *336*, 123.
- Cocke, D. L.; Johnson, E. D.; Merrill, R. P. *Catal. Rev.—Sci. Eng.* **1984**, *26*, 163.
- Moulder, J. F.; Stickle, W. F.; Sobol, P. E.; Bomben, K. D. In *Handbook of X-ray Photoelectron Spectroscopy*; Chastain, J., Ed.; Perkin-Elmer: Eden Prairie, MN, 1992.
- Chen, P. J.; Colaianni, M. L.; Yates, J. T. *Phys. Rev. B* **1990**, *41*, 8025.
- Wu, M.-C.; Goodman, D. W. *J. Phys. Chem.* **1994**, *98*, 9874.
- Thomas, T. D. *J. Electron Spectrosc. Relat. Phenom.* **1980**, *20*, 117.
- Kumar, K. V. *J. Electron Spectrosc. Relat. Phenom.* **1991**, *56*, 273.
- Schoen, G. *Acta Chem. Scand.* **1973**, *27*, 2623.
- Boronin, A. I.; Koscheev, S. V.; Zhidomirov, G. M. *J. Electron Spectrosc. Relat. Phenom.* **1998**, *96*, 43.
- Cai, Y. Q.; Bradshaw, A. M.; Guo, Q.; Goodman, D. W. *Surf. Sci.* **1998**, *399*, L357.
- Bao, X.; Muhler, M.; Schedel-Niedrig, Th.; Schlögl, R. *Phys. Rev. B* **1996**, *54*, 2249.
- Bielmann, M.; Schwaller, P.; Ruffieux, P.; Gröning, O.; Schlapbach, L.; Gröning, P. *Phys. Rev. B* **2002**, *65*, 235431.
- Tjeng, L. H.; Meinders, M. B. J.; van Elp, J.; Ghijsen, J.; Sawatzky, G. A.; Johnson, R. L. *Phys. Rev. B* **1990**, *41*, 3190.
- Schon, G. *Acta Chem. Scand.* **1973**, *27*, 2623.
- Bowker, M. *Surf. Sci.* **1985**, *155*, L276.
- Hoflund, G. B.; Hazos, Z. F.; Salaita, G. N. *Phys. Rev. B* **2000**, *62*, 11126.
- Weaver, J. F.; Hoflund, G. B. *J. Phys. Chem.* **1994**, *98*, 8519.
- Park, K. T.; Novikov, D. L.; Gubanov, V. A.; Freeman, A. J. *Phys. Rev. B* **1994**, *49*, 4425.
- Richter, B.; Kuhlbeck, H.; Freund, H.-J.; Bagus, P. S. *Phys. Rev. Lett.* **2004**, *93*, 26805.
- Santra, A. K.; Goodman, D. W. *J. Phys.: Condens. Matter* **2002**, *14*, R31.
- Wertheim, G. K.; DiCenzo, S. B.; Buchanan, D. N. E. *Phys. Rev. B* **1986**, *33*, 5384.
- Bagus, P. S.; Brundle, C. R.; Pacchioni, G.; Parmigiani, F. *Surf. Sci. Rep.* **1993**, *19*, 265.
- Wertheim, G. K. *Phys. Rev. B* **1987**, *36*, 9559.
- Yang, D. Q.; Sacher, E. *Appl. Surf. Sci.* **2002**, *195*, 187.
- Schmeisser, D.; Böhme, O.; Yafantis, A.; Heller, T.; Batchelor, D. R.; Lundstrom, I.; Spetz, A. L. *Phys. Rev. Lett.* **1999**, *83*, 380.
- Sun, C. Q. *Phys. Rev. B* **2004**, *69*, 45105.
- Sun, C. Q.; Pan, L. K.; Fu, Y. Q.; Tay, B. K.; Li, S. J. *Phys. Chem. B* **2003**, *107*, 5113.
- Sun, C. Q.; Tay, B. K.; Fu, Y. Q.; Li, S.; Chen, T. P.; Bai, H. L.; Jiang, E. Y. *J. Phys. Chem. B* **2003**, *107*, 411.
- Barth, J. V.; Zambelli, T.; Winterlin, J.; Schuster, R.; Ertl, G. *Phys. Rev. B* **1997**, *55*, 12902.
- Gravil, P. A.; White, J. A.; Bird, D. M. *Surf. Sci.* **1996**, *352*, 248.
- Pan, J. M.; Madey, T. E. *J. Vac. Sci. Technol., A* **1993**, *11*, 1667.
- Zhou, J.; Kang, Y. C.; Chen, D. A. *J. Phys. Chem. B* **2003**, *107*, 6664.
- Zhou, J.; Kang, Y. C.; Ma, S.; Chen, D. A. *Surf. Sci.* **2004**, *562*, 113.
- Schalow, T.; Brandt, B.; Starr, D. E.; Laurin, M.; Schauer mann, S.; Shaikhutdinov, S. K.; Libuda, J.; Freund, H.-J. *Catal. Lett.* **2006**, *107*, 189.
- Schalow, T.; Brandt, B.; Starr, D. E.; Laurin, M.; Shaikhutdinov, S. K.; Schauer mann, S.; Libuda, J.; Freund, H.-J. *Angew. Chem., Int. Ed.* **2006**, *45*, 3693.
- Bauer, E. Z. *Kristallogr.* **1958**, *110*, 372.
- Egelhoff, W. F., Jr. In *Ultrathin Magnetic Structures I, An Introduction to Electronic, Magnetic, and Structural Properties*; Bland, J. A. C., Heinrich, B., Eds.; Springer-Verlag: Berlin, Germany, 1994.
- Persaud, R.; Madey, T. E. In *Growth and Properties of Ultrathin Epitaxial Layers*; King, D. A., Woodruff, D. P., Eds.; Elsevier Science B. V.: New York, 1997.
- Mezey, L. Z.; Giber, J. *Jpn. J. Appl. Phys.* **1982**, *21*, 1569.
- Vitos, L.; Ruban, A. V.; Skriver, H. L. *Philos. Mag. B* **1998**, *78*, 487.
- Chambers, S. A. *Surf. Sci. Rep.* **2000**, *39*, 105.